Food Control 183 (2026) 111946

Contents lists available at ScienceDirect

Food Control

journal homepage: www.elsevier.com/locate/foodcont

A novel approach to confirm high-pressure processing and enhance traceability of meat products using near-infrared spectroscopy

Emanuela Zanardi [a], Maria Olga Varrà [a,*], Alessandra Negri [b], Riccardo Ghidini [b], Riccardo Soldesti [b], Adriana Ianieri [a], Sergio Ghidini [c]

[a] Department of Food and Drug, University of Parma, Strada del Taglio 10, 43126, Parma, Italy
[b] SterilParma S.p.A., Via Filagni 1, Collecchio, 43044, Italy
[c] Department of Veterinary Medicine and Animal Sciences, University of Milan, Via dell' Università 6, Lodi, 26900, Italy

ARTICLE INFO

Keywords:
Dry-cured meat
Fingerprinting
Chemometrics
Authentication

ABSTRACT

A novel near-infrared (NIR) spectroscopy method was developed to verify high-pressure processing (HPP) in traditional Italian meat products. Dry-cured pressed hams (n = 24), entire hams (n = 20), and salamis (n = 20) were analyzed using a portable NIR instrument before (C), immediately after (T0), and 48 h post-HPP (T48). Orthogonal partial least square discriminant models showed high cross-validation performances (R^2X, R^2Y, $Q^2 >$ 0.80), clearly separating C from T (T0+T48) samples of all products. Minor spectral differences observed between T0 and T48 salamis indicated storage-related changes, but these did not compromise the discrimination between C and T samples. The NIR bands most effective in discriminating C from T samples were primarily associated with protein, water, and fat absorption. External validation confirmed the reliability of the method, yielding classification accuracies of 100 % for entire hams, 90.5 % for salamis, and 79.2 % for pressed hams. This optimized approach can enhance traceability and control procedures, upholds food safety standards for HPP-treated meat products, and provides benefits for both the food industry and regulatory authorities.

1. Introduction

High-pressure processing (HPP) is a non-thermal technology for food decontamination and preservation, able to inactivate pathogenic and spoilage microorganisms, thereby enhancing food safety and extending the shelf life of food (Aymerich et al., 2008; Bajovic et al., 2012; EFSA Panel on Biological Hazards, 2022). Today, HPP is applied across a wide range of food and beverage categories, including juices, fishery products, ready-to-eat (RTE) meals, infant foods, meat, and meat products (EFSA Panel on Biological Hazards, 2022). The global annual production of HPP products is estimated at roughly 400,000 tons, with meat products accounting for 25–30 % of the total processed food outputs (Bolumar et al., 2021). Among these, RTE dry-cured meat products, especially in convenient formats such as pre-sliced and pre-packed items, represent the majority (Bolumar et al., 2021).

HPP treatment involves subjecting food products to isostatic pressures of up to 600 MPa for short durations, typically 1–6 min. The pressure is uniformly applied using a refrigerated transmitting fluid, thereby ensuring non-thermal conditions that preserve the original sensory and nutritional qualities of foods while meeting consumer demand for minimally processed food options (Patazca et al., 2007; Rasanayagam et al., 2003). Before HPP treatment, food products are typically pre-packaged in vacuum-sealed, flexible, and compressible materials, allowing the process to be carried out within the final packaging. This approach prevents recontamination, enabling the production of safer and longer-lasting products (Barba et al., 2015; Georget et al., 2015; EFSA Panel on Biological Hazards, 2022).

From an economic perspective, adopting HPP technology provides European companies with a strategic advantage in the global market. Specifically, the application of HPP has relevance in meeting the stringent "zero tolerance" policy for *Listeria monocytogenes* in RTE foods enforced in many non-European countries, thereby enabling European

Abbreviations: 1D, first derivative; 2D, second derivative; 3D, third derivative; 4D, fourth derivative; C, control (HPP-untreated); CV, cross-validation; HPP, high-pressure processin; MSC, multiplicative scatter correction; NIR, near-infrared; OC, orthogonal component; OPLS-DA, orthogonal partial least square-discriminant analysis; PA, polyamide; PC, predictive component; PE, polyethylene; SNV, standard normal variate; T, HPP-treated; T0, HPP treated recorded at timepoint 0; T48, HPP treated recorded at timepoint 48 h; VIP, variable influence on projection.

* Corresponding author.
E-mail address: mariaolga.varra@unipr.it (M.O. Varrà).

https://doi.org/10.1016/j.foodcont.2025.111946
Received 1 October 2025; Received in revised form 21 November 2025; Accepted 25 December 2025
Available online 27 December 2025
0956-7135/© 2025 The Authors. Published by Elsevier Ltd. This is an open access article under the CC BY-NC-ND license (http://creativecommons.org/licenses/by-nc-nd/4.0/).

companies to export high-value and traditional meat products to important foreign markets like the United States, Japan, Canada, and Australia (Hereu et al., 2011; Rubio-Celorio et al., 2016). HPP is currently of particular interest also to the European swine industry due to its potential to mitigate the impact of African swine fever, whose rapid spread across Europe, including Italy, has led to significant international trade restrictions. In fact, early studies and ongoing research provide preliminary evidence that HPP can reduce virus titer in meat (Petrini et al., 2024).

In the European Union, the HPP treatment is considered within the broader category of "processing" that can be applied to foodstuffs, as defined by Regulation (EC) 852/2004 (European Commission, 2004). Therefore, procedures based on good hygiene practices and Hazard Analysis and Critical Control Point systems, as well as requirements for traceability and labelling, extend to HPP treated products. Traceability of HPP-treated meat products intended for export to non-EU countries primarily relies on documentary evidence. In Italy, this process involves recording the treatment details in traceability logs, along with the release of a veterinary health certificate by the local competent authority, which serves as official proof that the products have undergone the treatment (Italian Ministry of Health, 2022). However, this document-based system has limitations, as it depends on accurate record-keeping and lacks an objective means of verification. Consequently, the system is more susceptible to fraud and unintentional human error, posing challenges for ensuring compliance with international export standards.

Although HPP is often referred to as a mild technology, studies have shown that it can induce both chemical and physical modifications in meat products. Chemical changes are primarily attributed to protein denaturation, aggregation, and gelation (Simonin et al., 2012; Sun & Holley, 2010; Tintchev et al., 2013), as well as water loss (Fuentes et al., 2010; Fulladosa et al., 2009). Lipid oxidation may also occur, potentially due to increased iron accessibility from hemoproteins and disruption of cell membranes under pressure (de Oliveira et al., 2021; Bolumar et al., 2021). The resulting physical changes, which arise from these chemical modifications, primarily involve alterations in the original structural properties of the matrix. Together, these modifications affect the way the meat products interact with electromagnetic radiation, leading to changes in their optical properties (Hassoun et al., 2020).

Based on this evidence, there is potential for research aimed at developing instrumental methods that target these changes, which could then be used to objectively verify and certify HPP treatment in meat products. One promising technique for achieving this goal is represented by near-infrared (NIR) spectroscopy. This technique leverages the interactions between NIR light and the matrix being analyzed, providing comprehensive information on both its chemical composition and physical properties in the form of a unique spectral fingerprint. This technique is rapid, non-invasive, and cost-effective, offering significant benefits for meat companies in both product and process authentication and control. Additionally, the availability of miniaturized and portable NIR instruments makes it suitable for on-site inspections and official controls, meeting the requirements for real-time, direct analysis (Beć et al., 2020a).

Given this potential, the objective of the present study was to test the hypothesis that the chemical and physical changes in meat products resulting from HPP treatment can be detected using NIR spectroscopy. Specifically, the research aimed to evaluate for the first time whether NIR spectroscopy, applied via a handheld device directly through food packaging, could represent a reliable, innovative, and non-destructive tool for providing concrete evidence of HPP treatment of traditional Italian dry-cured hams and dry-fermented sausages.

2. Materials and methods

2.1. Sample description

Three types of traditional Italian meat products were investigated, consisting of: i) N = 24 pressed hams (dry-cured, boneless, pressed, presenting a rectangular parallelepiped shape and with a weight of approx. 5 kg each), all packaged under vacuum in a polyamide (PA)/polyethylene (PE) multilayer barrier film; ii) N = 20 entire hams (dry-cured, boneless, entire, presenting the classic leg-shape and with a weight of approx. 9 kg each), all packaged under vacuum in a PE/PA multilayer barrier film; N = 20 salami (dry fermented pork sausages, with a weight of approx. 8 kg each), all packaged under vacuum in a PE/PA multilayer barrier film.

Both pressed and entire hams were produced for European and non-European markets by local manufactures by processing thighs of heavy pigs through dry-salting and a 9–12 month ripening period. Salami samples were also produced by local manufacturers by drying/fermentation for approximately 60 days of minced (medium grain) pork muscle and fat (with added sea salt, dextrose, spices, sodium ascorbate, sodium nitrite, potassium nitrate, lactic acid starter culture, and garlic powder).

2.2. HPP treatment

All the samples were stored at refrigerated temperature (+4 °C) before being subjected to HPP treatment, which was performed using a large commercial scale unit (Hiperbaric, Burgos, Spain) located in the production facility of SterilParma S.p.A.– Certosa Salumi S.p.A. (Parma, Italy). The protocol, previously established and validated by the same company, involved loading products into baskets placed within a high-pressure chamber, where an isostatic pressure of 600 MPa was kept for 6 min using refrigerated water as the pressure-transmitting medium. This protocol is routinely employed by the company to process meat products in adherence to self-control and export procedures. Before and after HPP treatment, the samples were stored at a temperature below +4 °C. The temperature of the products immediately following HPP ranged from 15 to 18 °C.

2.3. NIR analysis

2.3.1. Experimental design

Given the naturally non-homogeneous structure of hams, which include different muscular sections, multiple measurement areas from pressed and entire ham surfaces were included within the experimental design for spectroscopic analysis (Fig. 1). These areas were carefully chosen to be free from visible fat, defects, and wrinkles in the packaging film. The objective was to identify the sample section that yielded the most robust and representative spectral data. For pressed hams, five measurement areas, namely "A", "B", "C", "D", and "E", were selected at the top (or specular bottom) surface of the parallelepiped block (Fig. S1, Supplementary Material). For entire hams, two exposed muscular sections (without rind and visible pork fat), namely "A" and "B", were selected (Fig. S2, Supplementary Material). Considering the more homogeneous composition of salamis, the identification of the best responding measurement area was considered less critical. However, for the sake of analysis standardization, the central area of each salami surface was systematically selected (Fig. S3, Supplementary Material). Every selected area underwent NIR analysis across three distinct stages (Fig. 1), namely: i) control (C) stage (post vacuum-packaging and just before the HPP treatment); ii) T0 stage (immediately following the HPP treatment; iii) T48 stage (48 h after the HPP treatment).

2.3.2. NIR instrumental measurement

NIR analysis covering the 908–1676 nm electromagnetic spectrum range was performed in diffuse reflectance mode using a portable and miniaturized device (MicroNIR On-Site W, Viavi Solutions). Each

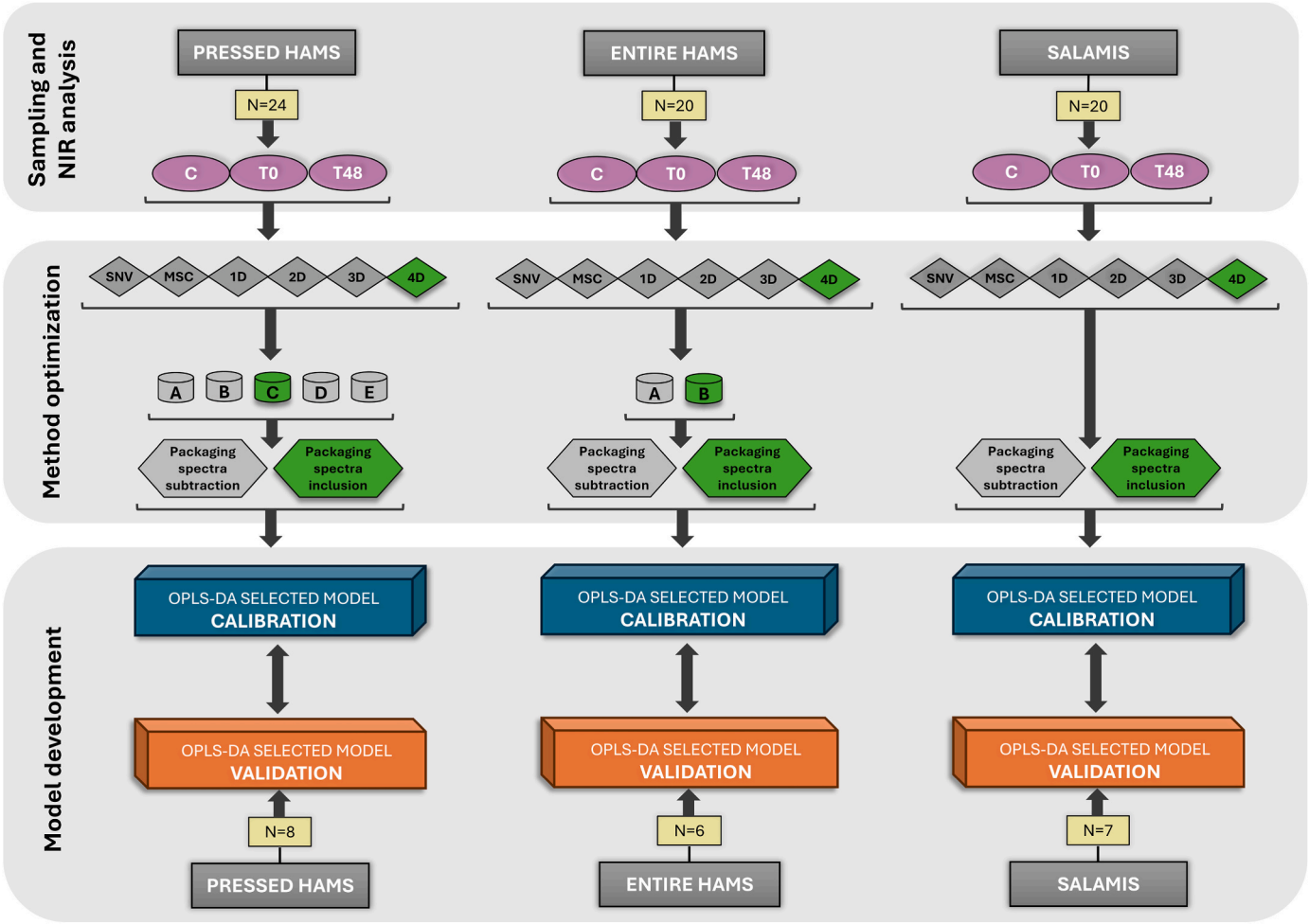


Fig. 1. Workflow of the experimental design for developing and validating discriminant models based on NIR spectral data to distinguish untreated and HPP-treated pressed ham, entire ham, and salami samples (1D = first derivative; 2D = second derivative; 3D = third derivative; 4D = fourth derivative; OPLS-DA = orthogonal partial least-squares discriminant analysis).

spectrum acquisition involved 100 co-added scans with an integration time of 100 ms and a resolution of 6.2 nm. Analyses were performed though the sample packaging by positioning the acquisition window of the spectrometer in direct contact with the surface of the sample. To account for potential variations arising from composition, four distinct spectral replicates were consecutively recorded for each section of the hams. As for salamis, ten distinct spectral replicates were instead recorded.

Representative NIR spectra were recorded also from the individual PA/PE multilayer packaging films used for vacuum wrapping the samples. For this purpose, three distinct films per type of meat product were analyzed, with ten spectral replicates recorded for each film. The device was placed in direct contact with the film surface, which was positioned on a white ceramic desk.

The spectral replicates collected for each meat sample were averaged prior to calculation to obtain a final averaged spectrum.

Instrumental calibration and background correction were periodically performed through the recording of a total absorbance (dark) spectrum and a total reflectance (white) reference spectrum, utilizing Spectralon® 99 % (LabSphere, North Sutton, NH, USA) as the standard reference material.

2.4. Methodological refinement for optimal chemometric modeling of NIR spectral data

The goal of applying chemometrics to the collected NIR spectra of meat products was to develop multivariate discriminant models to differentiate between C and T0/T48 samples. The complete raw data matrices subjected to chemometrics consisted of:

- N = 125 apparent absorbance values (log 1/R, 908–1676 nm) × 360 NIR spectra of pressed hams (24 samples × 5 measurement areas A, B, C, D, and E × 1 average NIR spectrum × 3 conditions C, T0, and T48);
- N = 125 apparent absorbance values (log 1/R, 908–1676 nm) × 120 NIR spectra of entire hams (20 samples × 2 measurement areas A and B, × 1 average NIR spectrum × 3 conditions C, T0, and T48);
- N = 125 apparent absorbance values (log 1/R, 908–1676 nm) × 60 NIR spectra of salami (20 samples × 1 average NIR spectrum × 3 conditions C, T0, and T48).

During the analytical workflow, three critical decision-making steps were identified and deeply investigated to refine the methodology and develop final robust calibration models aimed at effectively distinguishing between C and T (T0 + T48) meat products. These included the identification of the most effective methods to pre-process raw NIR spectral data, the determination of the optimal ham measurement area, and the assessment of the stability of the method in relation to the potential impact of the packaging material on the NIR spectra. These decision-making steps were addressed consecutively in sequential progression, as summarized in Fig. 1 and detailed in the following paragraphs. Initially, a broad exploration of various spectral pre-processing

techniques was conducted to identify the most effective approach. Following this, the optimal measurement areas of the hams were identified and selected. Finally, the impact of packaging was investigated by subtracting spectra of films to the spectra of samples. Each step in this process was contingent upon the findings and decisions made in the preceding stage and contributed to the methodical refinement of the overall process prior to the development of the final C vs. T discriminant models. Chemometric elaborations were all performed using the SIMCA® software (v. 17.0.2.34594, Sartorius Stedim Data Analytics AB, Umea, Sweden).

2.4.1. Pre-processing of NIR spectral data

To enhance the quality of the spectral data before performing further analysis, pre-processing techniques including standard normal variate (SNV), multiplicative scatter correction (MSC), and first (1^{st}) to fourth (4^{th}) order derivatives, were either applied individually or in combination to raw NIR spectra of ham and salami data matrices. Several multivariate discriminant models based on orthogonal partial least squares-discriminant analysis (OPLS-DA) comparing the differently pre-processed spectra of C versus T (T0 + T48) hams or salami were then generated. The optimal pre-processing method was selected based on a combination of visual inspection of the quality of the pre-processed spectra and evaluation of statistical outputs from 7-fold cross-validation (CV) of the resulting OPLS-DA models. Key classification performance metrics consisting of R^2Y and Q^2 values were assessed, with higher values indicating superior model performance.

2.4.2. Determination of the optimal ham measurement area

The most informative and effective ham portion (i.e., the ham muscular segment at surface giving the best discrimination outputs) was studied and identified. To this end, various OPLS-DA models were developed, using the best pre-processed spectra previously selected (Fig. 1). Each model was constructed by incorporating NIR spectra recorded at a single acquisition point per time, i.e., spectra of areas A, B, C, D, and E of pressed hams, and from areas A and B of entire hams (see Section 2.3.1 Experimental design). The optimal ham measurement area was therefore selected based on the predictive performance metrics R^2Y and Q^2 values resulting from 7-fold CV of the C vs. T OPLS-DA models.

2.4.3. Evaluation of the influence of the packaging material

An investigation was also undertaken to assess the impact of the external packaging materials on the overall spectral characteristics of samples. The goal was to account for any potential interference deriving from the absorption of the NIR radiation by the PA/PE polymer, which could compromise the accuracy and robustness of the discriminant models. To achieve this, new NIR data matrices were generated by mathematically subtracting the average raw NIR spectrum of the plastic films used for wrapping pressed hams, entire hams, or salami from the respective raw NIR spectra of the whole products (i.e., data recorded through the packaging). The resulting subtracted spectra, thus representing the NIR spectra of the "meat only," were then pre-processed using the same optimal algorithm previously selected and subjected to OPLS-DA. The performance of the resulting C vs. T models was assessed by evaluating the statistical predictive parameters R^2Y and Q^2 values obtained by 7-fold CV as compared to those obtained of the models generated using the spectra recorded through the packaging.

2.4.4. Calibration and validation of the optimized discriminant models

Once selected the best pre-processing algorithm, the best ham surface responding area, and the feasibility of using spectra encompassing packaging absorption contributions, the final NIR data matrices for pressed hams, entire hams, and salami to be used for the calibration of the final OPLS-DA model included: N = 72 NIR spectra of pressed hams (24 samples × 1 selected designated measurement area × 1 average NIR spectrum × 3 conditions C, T0, and T48); N = 60 NIR spectra of entire hams (20 samples × 1 selected designated measurement area × 1 average NIR spectrum × 3 conditions C, T0, and T48); N = 60 NIR spectra of salami (20 samples × 1 average NIR spectrum × 3 conditions C, T0, and T48).

Final calibration models were internally validated using 7-fold CV to reduce the risk of overfitting and overprediction, and their reliability assessed though the evaluation of R^2X, R^2Y, and Q^2 parameters. Overfitting and overprediction of the calibration models were also excluded through a permutation test (using 400 random permutations) and by evaluating the resulting permuted R^2X and Q^2 parameters. The *y*-intercepts of these parameters should be lower than those of the calibration models for R^2X and negative for Q^2 to confirm model validity. Potential outlier samples were identified through visual inspection of the individual sample and by performing an Hotelling's T^2 test ($p \leq 0.05$).

The variable influence on projection (VIP) analysis was performed to identify the NIR absorption bands that contributed most to the differentiation between samples. To this end, VIP indices for the predictive fraction of the OPLS-DA models with values ≥ 1.0 were considered significant (Galindo-Prieto et al., 2015).

Finally, to assess the effectiveness of the calibration models under real-world conditions, the models were tested against new samples employed as external validation sets. The validation sets, designed to include approximately 25 % of the samples used for model calibration, comprised C and T NIR spectra from N = 8 pressed hams, N = 6 entire hams, and N = 7 salamis, all collected from distinct product batches at different times (Fig. 1). Validation samples were measured using the same analytical conditions detailed in Section 2.3. and pre-processed to align to the calibration samples following the same procedure reported in Section 2.4.1. The outputs of the external validation process were evaluated by analyzing the resulting confusion matrices.

3. Results and discussion

3.1. Insights from methodology optimization

The initial step of the method optimization involved evaluating various pre-processing techniques to identify the most effective approach for improving the quality of raw NIR spectra.

The results obtained showed that the 4^{th}-order derivative was the most suitable technique for pre-processing the raw spectral data of all three types of meat products. Indeed, when applied independently, 4^{th}-order derivative method allowed to generate OPLS-DA models with the highest R^2Y and Q^2 values, both of which were found to be above 0.814 (Table S1, Supplementary Material). In contrast, applying the 1^{st}-order derivative method resulted in the poorest performance, and combining derivatives with scattering correction techniques such as SNV and MSC failed to enhance the outputs of the discriminant models (Table S1, Supplementary Material). The effectiveness of the 4^{th}-order derivative preprocessing technique was further confirmed through visual inspection of the resulting NIR spectra, which appeared free from apparent artificial noise (Fig. S2, Supplementary Material). Based on this evidence, the 4^{th}-order derivative was selected as the optimal pre-processing method and used in the chemometric analysis of the data from this point onward. The superior performance of the 4^{th}-order derivative can be ascribed to its ability to accentuate sharp peaks and subtle spectral variations, which are often hidden in raw NIR spectral data but essential for distinguishing complex matrices like meat products (Niemeyer et al., 2010). These subtle spectral features were critical for differentiating C from T samples, suggesting that while variations related to HPP treatment were present in the spectra, they were minimal and required advanced pre-processing techniques to be uncovered.

These findings are not always consistent with literature. For example, applying MSC to NIR spectra of minced meat of pork sausages produced better predictive results than derivative techniques, likely due to its superior ability in handling light scattering effects arising from the physical structure of the sausages (Ritthiruangdej et al., 2011).

However, since there are no universal guidelines for mathematical correction of NIR spectra, different preprocessing techniques should always be tested for each food matrix to identify the most appropriate method for the specific product (Ritthiruangdej et al., 2011).

In a second instance, the analysis of spectral data from different measurement areas of the hams revealed that sampling location significantly influenced the performance of the predictive models, with certain regions exhibiting spectral characteristics that were more effective in distinguishing HPP-treated samples. For pressed hams, the use of spectra recorded from the central area, labelled as "C" (Fig. S1A, Supplementary Material), provided the best prediction results, with $R^2Y = 0.931$ and $Q^2 = 0.845$ (Table S2, Supplementary Material). This result may be explained by the fact that the central area of the pressed ham provided clearer spectral data, likely due to reduced interference from external factors. Indeed, the more peripheral areas ("A", "B", "D", and E) often contained wrinkles in the packaging generated during the vacuum process and which may have introduced additional variability into the measurements that obscured subtle differences between C and T samples. It is also noteworthy that considerable structural variability was observed among the different pressed ham specimens analyzed. This variability likely resulted from the pressing process used to shape the ham into a brick form and was mainly due to differences in muscle orientation and positioning, which introduced inconsistencies.

For entire hams, the measurement area "B" yielded better predictive outcomes ($R^2Y = 0.888$, $Q^2 = 0.800$, Table S2 of the Supplementary Material) compared to area "A" (Fig. S1B, Supplementary Material). Similar to pressed hams, this result may be attributed to higher spectral variability observed in area "A," which was characterized by the juxtaposition of different muscle types and varying muscle orientations across specimens. Additionally, variations in trimming between samples, along with factors such as the presence of tyrosine crystals on the surface, may have further contributed to spectral distortion and reduced reproducibility. All these factors have been previously identified by other researchers as significant sources of unwanted spectral variation in hams and other meat products (Collell et al., 2011; Prieto et al., 2009).

Therefore, based on these results, only the NIR spectra recorded from surface area "C" of the pressed hams and the surface area "B" of the entire hams were selected for the development of the final discriminant models.

At the third and final stage of the method optimization workflow, results and insights were gathered regarding the impact of the packaging material on the stability and consistency of the NIR spectra. The raw spectra of the three packaging materials, corresponding to the films used to wrap pressed hams, entire hams, and salami samples, are presented in Figs. S3A, S3B, and S3C (Supplementary Material). Upon visual inspection, they displayed consistently homogeneous and reproducible absorption patterns, with distinct peaks observed in the 908–1686 nm range, indicating their ability to absorb NIR electromagnetic radiation. However, these peaks were significantly less intense compared to those from the meat products themselves (Figs. S2A, S2B, and S2C, Supplementary Material). This suggests that the spectral signals from packaging were minimal and unlikely to interfere with those associated with meat absorption. This initial observation was further confirmed by assessing the performance of new OPLS-DA models generated using NIR spectra obtained after subtraction of the absorbance of the packaging. As shown in Table S3 (Supplementary Material), the new discriminant models generated using the subtracted spectra did not show significant improvement in performance when compared to those using the full NIR spectra of samples (which included absorbance from the packaging material). Hence, the spectral contributions from the packaging did not distort their predictive power. Given this, it was concluded that incorporating the absorbance from the packaging into the final discriminant models was more appropriate than attempting to subtract it out.

Scientific literature consistently supports the use of NIR spectroscopy through packaging for analyzing the surface of meat and meat products, strongly emphasizing the advantages of its non-invasive nature. For instance, it has been demonstrated that the predictive accuracy for determining the chemical composition of pork sausages remained consistent whether NIR spectra were collected directly from the sausage surface or through the packaging (Ritthiruangdej et al., 2011). Similarly, the performance of chemometric models for detecting pork adulteration showed no significant differences when spectra were recorded from unpackaged samples or through polymer packaging (Schmutzler et al., 2015). Comparable results were also reported for freshness assessment of packaged pork loin slices (Arias et al., 2022; Tejerina et al., 2021), packaged and unpackaged dry-cured hams (León et al., 2023), and HPP-treated ham slices (Pavli et al., 2018).

3.2. Final discriminant models: untreated vs. HPP-treated meat products

3.2.1. NIR spectral patterns

The average NIR spectra of C and T pressed hams, entire hams, and salamis used for the calibration of the final OPLS-DA model are presented in Fig. 2A, B, and 2C, respectively. As expected, pressed and entire hams exhibited similar spectral signatures, since they were composed by the same type of food matrix. However, slight differences in overall peak intensities were observed, likely related to variations in light scattering caused by differences in structural characteristics between these products. Both sample types showed prominent negative peaks in the 1110–1150 nm, 1180–1200 nm, 1230–1260 nm, and 1360–1390 nm regions (Fig. 2A and B), which are typically associated with hydrocarbon absorption (Workman & Weyer, 2012). Although from the visual-only analysis of the spectra substantial differences in terms of peak intensity or spectral line patterns were hardly perceivable, it was observed that in the case of pressed hams, peaks centered at approximately 1190 nm, 1240 nm, and 1380 nm were visibly pronounced in C compared to T samples (Fig. 2A). For entire hams, these differences were less evident (Fig. 2B). Overall, the spectral patterns and intensities observed in this study are consistent with those reported in previous research on dry-cured hams analyzed using the same portable NIR instrument (Hernández-Jiménez et al., 2024).

With regard to salamis, the recorded NIR spectra (Fig. 2C) were very similar to those reported in the literature for dry-fermented sausages by González-Mohino and colleagues (González-Mohino et al., 2020). Compared to hams, broader variations in peak curvature and intensity were observed (Fig. 2C), which can be attributed to their significantly different physical properties and chemical composition, including a higher fat content and lower moisture levels. The lower moisture content, in particular, is associated with a reduced absorption intensity and overlap of NIR bands of water, thereby enabling sharper and more distinct peaks from other components to be observed (Fig. 3C). As with hams, the most prominent peaks were observed in the regions around 1110–1150 nm, 1180–1200 nm, and 1230–1260 nm (Fig. 2C). Among these, the peaks centered at 1190 nm and, particularly, at 1240 nm were more pronounced, while the peak at 1380 nm was less intense compared to the corresponding peaks in hams.

3.2.2. Results from cross-validation

The score plots of the OPLS-DA calibration models developed and internally validated (7-fold CV) discriminating C vs. T pressed hams, entire hams, and salamis are presented in Fig. 3A, B, and 3C, respectively. These plots illustrate the distribution of samples in the three-dimensional space defined by the first predictive component (PC1) and the first two orthogonal components (OC1 and OC2). As shown, distinct clusters for C and T samples were observed along the PC1 for all the meat products, even though a certain degree of intraclass variability was captured along OC1 and OC2. Samples falling outside the 95 % confidence interval (indicated by the ellipse) were not identified as strong outliers according to Hotelling's T^2 statistics. Moreover, a visual inspection of their NIR spectra showed no anomalies, so they were not excluded.

When analyzing the statistical outputs, it was found that the pressed

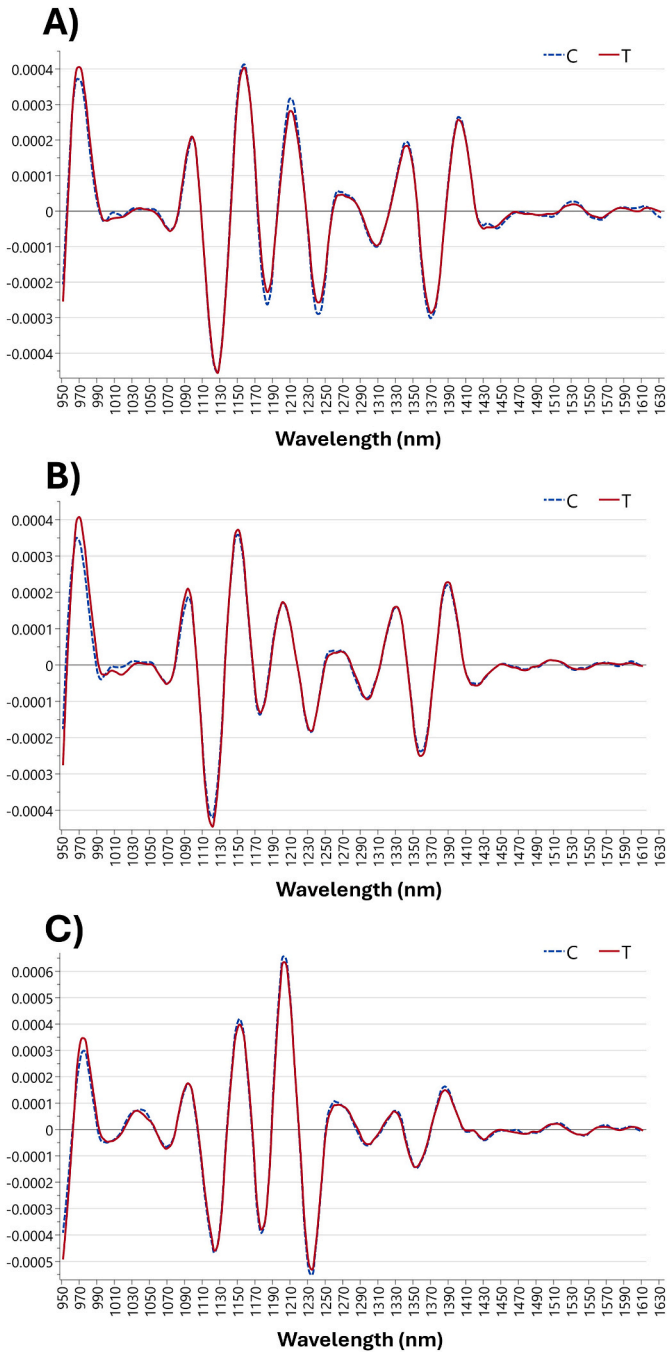


Fig. 2. Average 4th-order derivative NIR spectra (908–1676 nm range) of pressed hams (**A**), entire hams (**B**), and salamis (**C**) collected from untreated (control, C) and HPP-treated (treated, T) samples.

ham calibration model demonstrated a high fitting ability (R^2X = 0.993), along with excellent predictive performance ($R^2Y = 0.931$, Q^2 = 0.845) (Table 1). Additionally, the model showed no signs of overfitting or overprediction, as confirmed by R^2X - *y*-intercept being lower than R^2X and negative Q^2 - *y*-intercept values (Table 1). These metrics, coupled with the distinct separation between C and T samples (Fig. 3A), collectively underscored the potential effectiveness of the model.

The model for entire hams (Fig. 3B) also displayed satisfactory performance, with $R^2X = 0.845$, $R^2Y = 0.888$, and $Q^2 = 0.800$ (Table 1). Although the predictive ability was slightly lower compared to that of the pressed hams, the distinct clustering of C and T samples along the PC1 confirmed its discrimination ability (Fig. 3B). A sub-clustering of T

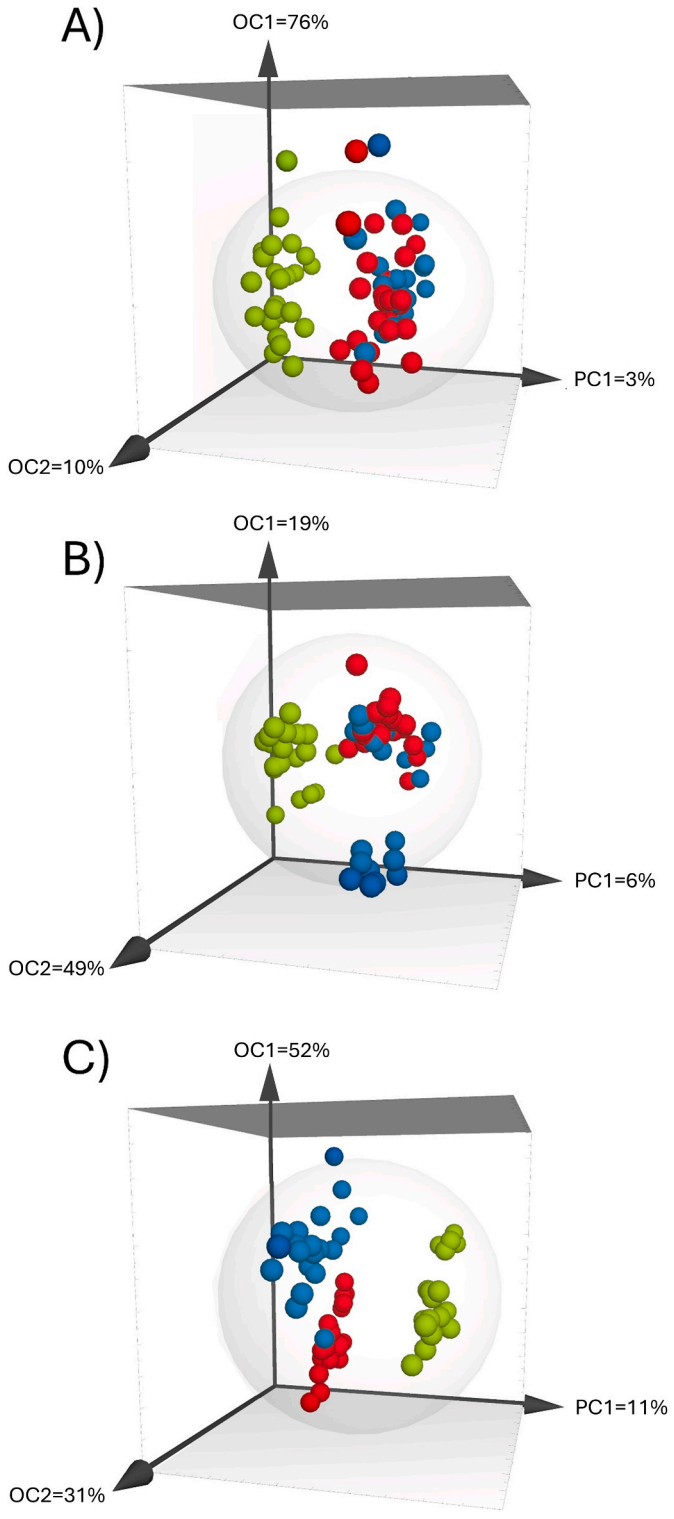


Fig. 3. Score scatter plots showing the spatial distribution of untreated (control, C; green spheres) and HPP-treated (treated, T; T0 as blue spheres and T48 as red spheres) pressed hams (**A**), entire hams (**B**), and salamis (**C**) along the first predictive component (PC1) and the first two orthogonal components (OC1, OC2) of the corresponding OPLS-DA calibration models. (For interpretation of the references to color in this figure legend, the reader is referred to the Web version of this article.)

Table 1
Performance metrics of the OPLS-DA calibration models developed for untreated (C) and HPP-treated (T) pressed hams, entire hams, and salamis.

	Pressed hams		Entire hams		Salamis	
Sample class	C	T	C	T	C	T
Comp.	1 + 9		1 + 4		1 + 5	
R^2X	0.993		0.845		0.987	
R^2Y	0.931		0.888		0.986	
Q2	0.845		0.800		0.972	
R^2X - *y*-intercept	0.402	0.397	0.271	−0.650	0.229	−0.561
Q^2 - *y*-intercept	−0.806	−0.796	0.274	−0.643	0.222	−0.579

Comp = number of predictive + orthogonal components. R^2X = cumulative proportion of variance in the predictor variables (X) explained by the model; R^2Y = cumulative proportion of variance in the response variable (Y) explained by the model; Q^2 = cumulative prediction ability of the model to predict new data; R^2X - *y*-intercept = intercept on the *y* axis of the R^2X obtained during the permutation test (400 permutations) indicating the variance in predictor variables (X) explained by the model when random data is used; Q^2 - *y*-intercept = intercept on the *y* axis of the Q^2 obtained during the permutation test (400 permutations) indicating the cumulative prediction ability of the model when random data is used.

samples recorded immediately after HPP treatment (T0) was also observed, suggesting that these samples acquired distinct optical properties post-treatment. However, after storage (T48), these samples clustered together with other T0 samples, indicating that any immediate changes in optical properties induced by HPP treatment tended to disappear or stabilize over time.

For salamis, the OPLS-DA model was characterized by a high fitting ($R^2X = 0.987$) and the best predictive abilities ($R^2Y = 0.986$, and $Q^2 = 0.972$) (Table 1), which resulted in a more pronounced separation between C and T samples along the PC1 of the score plot (Fig. 3C). This outcome can be attributed to the well-documented evidence that minced samples are characterized by a more homogeneous matrix which enhances the interaction between NIR light and the material (Cáceres-Nevado et al., 2019; De Marchi et al., 2017; Fernández-Barroso et al., 2021). From the visual analysis of the score plot (Fig. 3C), a clear internal separation between T0 and T48 salami samples was also evident. This may suggest that, compared to hams, the salami matrix is more sensitive to time-dependent physicochemical changes following HPP treatment. Nevertheless, it is important to emphasize that this separation effect did not negatively impact the primary objective of this study, as they did not introduce variability that would hinder the discrimination between C and T samples (i.e., both T0 and T48 samples clustered together in the right part of the plot, far away from C samples). Hence, this result, obtained by including NIR spectra of both T0 and T48 samples, can be regarded as very promising, as it demonstrates that the model effectively accounted for unwanted spectral variations and maintained reliable discrimination performance despite post-processing changes.

Globally, the separation of both T0 and T48 samples from C samples of both hams and salamis confirms that, when present, HPP-induced changes across all analyzed food matrices are stable and not reversible. Consequently, the robustness of the method can be regarded as improved, and its applicability broadened, enabling its potential use also at various stages of the shelf life of the investigated meat products.

Previous studies have reported that changes in the meat matrix following HPP treatment are generally stable, with no further significant modifications occurring during long-term storage. For example, HPP of beef and lamb led to increased lightness and yellowness and reduced redness immediately after treatment, with no additional color changes observed throughout storage (McArdle et al., 2011; McArdle et al., 2013). In contrast, other studies reported that differences in color attributes and the extent of lipid and protein oxidation of HPP-treated meat products gradually diminished over the storage period (Campus et al., 2008).

3.2.3. Results from VIP analysis

VIP analysis was performed to identify the NIR absorption bands most influential in separating C and T samples, enhancing the interpretability of the results. Fig. 4A, B, and 4C show the predictive VIP indices for pressed hams, whole hams, and salami, respectively.

For pressed hams (Fig. 4A), the most significant variables (VIP >2.7) were identified as the absorption bands located within the 1174–1190 nm range. NIR peaks falling within this region have been previously associated with the third overtone of the C–H stretching vibration in alkenes (HC=CH groups) and methyl C–H groups in aliphatic hydrocarbons (Workman & Weyer, 2012). Lower, yet still substantial, VIP values (VIP >2.3) were observed for wavelengths in the 1200–1260 nm range, where combination bands corresponding to the O–H stretching vibrations from water and the C–H bending vibrations of C–H rich compounds were reported (Beć et al., 2020b; Workman & Weyer, 2012). Additionally, high VIP values were observed in the 950–1000 nm region (VIP >2.2), where the absorption bands are primarily associated with the third overtone of the O–H stretching vibration, typical of alkyl alcohols or, more commonly, water (Workman & Weyer, 2012).

The VIP profile for entire hams (Fig. 4B) differed significantly from that of pressed hams, despite the similarities in the composition of the two meat products. The NIR wavelengths exhibiting high VIP values (VIP >2) were primarily located in the 1470–1490 nm and 1500–1520 nm ranges, where absorption bands are associated with N–H stretching vibrations from urea, primary amides, proteins, primary aromatic amines, and secondary amines (Beć et al., 2020b; Workman & Weyer, 2012). Peaks in the 1540–1580 nm range were also significant (VIP >2.2), previously assigned to both the N–H stretching vibrations of secondary amines and the O–H stretching vibrations of water. NIR bands in the 1590–1620 nm region (VIP >1.5) can be attributed to the C–H stretching vibrations of the C=O group in ketones, while those in the 1000–1050 nm range are associated with the O–H and C–O stretching vibrations of ethers and esters, N–H stretching vibrations from primary aromatic amines, and C–H stretching vibrations from aliphatic hydrocarbons (Workman & Weyer, 2012).

The VIP indices for salamis (Fig. 4C) were more similar to those of pressed hams than to those of entire hams. For salamis, the highest VIP values were observed for NIR bands associated with water in the 950–1000 nm region (VIP >2.5), as well as bands in the 1190–1220 nm region (VIP >1.5, attributable to C–H stretching vibrations of aliphatic hydrocarbons and O–H stretching from water, and the 1230–1250 nm region (VIP >1.5, associated with C-H stretching vibrations of aliphatic hydrocarbons) (Beć et al., 2020b; Workman & Weyer, 2012).

Despite some differences, all the above outcomes highlight modification of water, nitrogen-containing, and fat-related compounds as key contributors to sample discrimination, confirming that NIR spectroscopy can effectively distinguish between HPP-treated meat products as detectable variations in the main constituents occur following treatment. Supporting these findings, a previous study on pork samples pressurized at 200, 400, 600, and 800 MPa reported significant NIR spectral variations linked to the treatment as being predominantly associated to water and protein absorption (Grossi et al., 2016). The authors attributed these changes to the proteolytic fragmentation of the myofibrils and protein aggregation induced by HPP, which led to alterations in matrix properties through the disruption and formation of new interactions between proteins and water molecules (Grossi et al., 2016). Many other studies confirm a strong influence of pressure on the unfolding of both tertiary and quaternary structures of muscle proteins at pressures above 200 MPa, with denaturation, gel formation, and protein agglomeration occurring at even higher-pressure values (Bajovic et al., 2012; Bolumar et al., 2021; Picouet et al., 2012). In contrast, the impact of pressurization on lipids is still less understood, but existing literature suggests that oxidation may be enhanced, likely due to increased iron availability from hemoproteins and membrane disruption (Bajovic et al., 2012; de Oliveira et al., 2017). Finally, modifications in the alcohol, ketone, and ester contents of meat products have also been

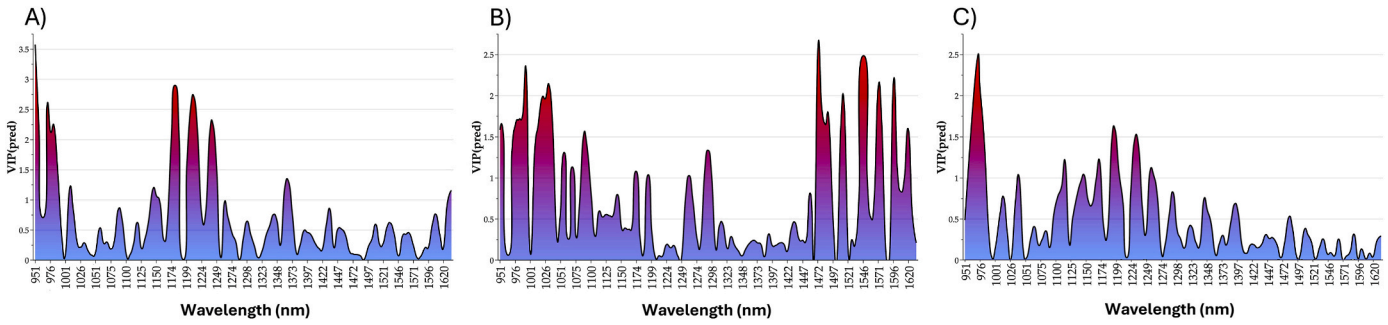


Fig. 4. Variable influence on projection (VIP) indices of NIR wavelengths contributing to the discrimination of untreated and HPP-treated pressed hams (**A**), entire hams (**B**), and salamis (**C**). The color gradient from blue to red indicates increasing significance, with VIP ≥1.0 as the threshold. (For interpretation of the references to color in this figure legend, the reader is referred to the Web version of this article.)

attributed to HPP treatment. However, drawing definitive conclusions regarding the effectiveness of NIR spectroscopy in capturing spectral changes specifically associated with these compounds can be made with significantly less confidence, due to the well-known low sensitivity of this technique (Pérez-Santaescolástica et al., 2019).

3.2.4. *Results from external validation*

While CV is a useful technique, it may not always be sufficient to assess the robustness and generalizability of discriminant models. To address this, external validation was performed using separate sets of new C and T samples. The results of the external validation are summarized in the confusion matrices shown in Fig. 5.

Overall performance varied significantly across sample types. A perfect classification accuracy (100 %) was achieved for entire hams (Fig. 5B), where all validation samples were correctly recognized without error. For salami samples (Fig. 5C), a promising, though not perfect, correct classification rate of 90.5 % was observed, due to the misclassification of one C sample as T and one T sample (specifically a T0 sample) as C.

For pressed hams (Fig. 5A), the model achieved an overall correct classification rate of 79.2 %. Despite high performance during CV of the calibration set (Table 1), only 5 out of 8 C samples and 14 out of 16 T samples were correctly identified, resulting in 37.5 % of C samples being misclassified as T. A closer examination revealed that the two T pressed hams incorrectly classified as C were both analyzed immediately after HPP treatment (T0). Although their NIR spectra were recorded on the same day, these misclassified T0 samples underwent two independent HPP processes and originated from distinct production batches, albeit being produced by the same Italian company. This suggests that the lower classification accuracy for pressed hams may arise from some spectral similarity between C and early-stage T samples, whereas these confounding similarities likely diminish over time. Nevertheless, this markedly lower accuracy indicates that the pressed ham model currently has limited reliability for routine control or traceability purposes, as its direct implementation could lead to practical drawbacks. For instance, the misclassification of T samples as C could lead to unnecessary rejections, while the more critical misclassification of C samples as T could pose significant risks to food safety due to potential pathogens spread.

Overall, some hypotheses can be proposed to explain the reduced performance observed for pressed hams, with their inherently higher structural and compositional variability likely representing the main contributing factor. Pressed hams undergo deboning, trimming, and mechanical pressing, operations that alter the native orientation of muscle groups and fibers and create more variable sub-surface distributions of fat and connective tissue compared to entire hams. Such factors introduce spectral variability unrelated to HPP treatment, thereby reducing discrimination performance. To address this limitation, it is evident that further methodological refinement is required before the discriminant model can be recommended for operational use. In this regard, testing a broad panel of standard spectral pre-processing methods did not yield meaningful improvements, indicating that spectral correction alone cannot compensate for the structural complexity of this matrix. Alternatively, it may be hypothesized that more advanced non-linear chemometric or machine-learning approaches may better capture non-linear patterns in NIR spectra and improve performance; however, such methods demand greater computational resources and

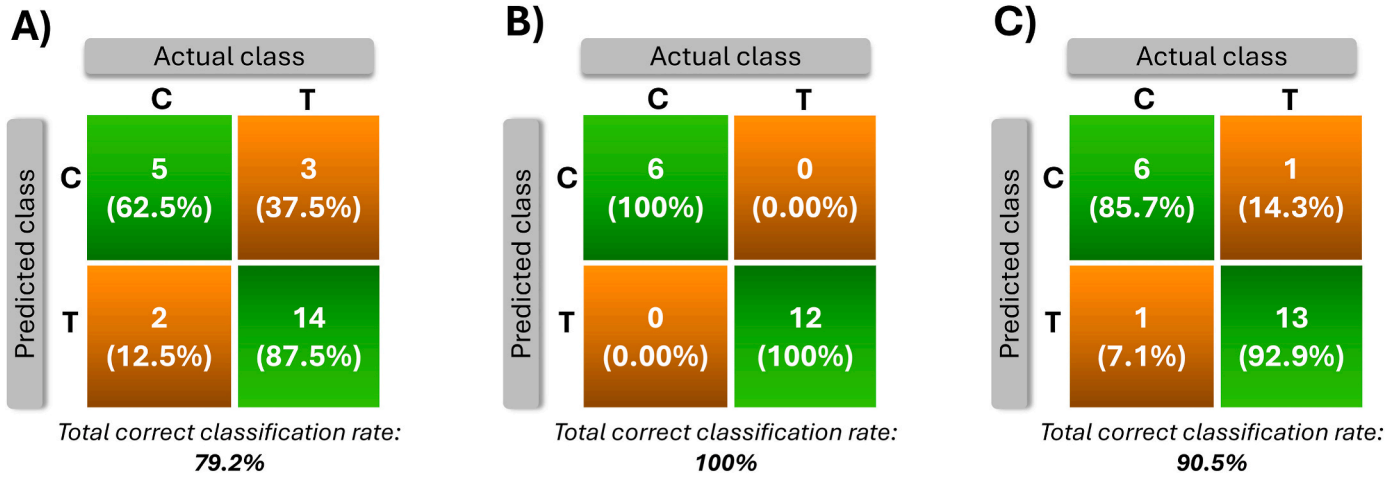


Fig. 5. Confusion matrices resulting from the external validation of the OPLS-DA models for untreated (control, C) and HPP-treated (T, treated) pressed hams (**A**), entire hams (**B**), and salamis (**C**). Correctly classified and misclassified validation samples are included in green and orange boxes, respectively. (For interpretation of the references to color in this figure legend, the reader is referred to the Web version of this article.)

are not always implementable within the software environment of the MicroNIR device. Within these constraints, it can be confidently stated that expanding the calibration and validation datasets currently represents the most realistic and effective strategy for improving robustness and accuracy, as larger sample sets would better represent the inherent variability of pressed hams and improve discrimination between C and T samples.

To the best of the authors' knowledge, no prior applications of NIR spectroscopy as a rapid method for verifying HPP treatment in food have been reported. Therefore, direct comparisons with existing literature or further contextualization of the findings are not feasible. Although NIR spectroscopy is well established for assessing chemical composition, quality, and authenticity attributes of food matrices, its use in monitoring processing or technological treatments remains limited. In this context, vibrational spectroscopic techniques such as Raman and fluorescence spectroscopy have been successfully applied to monitor heat treatments in milk and other dairy products, owing to their ability to detect heat-induced matrix modifications (Mungkarndee et al., 2016; Reiner et al., 2020; Yazgan et al., 2020). For meat products, NIR spectroscopy has only been applied to verify irradiation in dry fermented sausages, where it successfully distinguished irradiated from non-irradiated samples despite the minimal spectral differences associated with treatment (Varrà et al., 2020).

All these applications highlight the considerable potential for extending the use of NIR spectroscopy to monitor HPP treatments in food. Therefore, further exploration in this area is strongly encouraged, as it could provide significant advancements in the field of food authenticity and safety monitoring.

4. Conclusions

This study provides preliminary evidence supporting the potential of NIR spectroscopy as a fast and non-destructive method for verifying HPP treatment in traditional Italian meat products. The optimized approach allowed to differentiate untreated and HPP-treated samples across various products, including dry-cured hams and dry-fermented sausages, offering a practical solution to meet strict food safety, inspection, and traceability standards.

The implementation of this methodology could offer a range of significant benefits. For food business operators, it may serve as a non-invasive and portable tool to enhance own-check procedures by moving beyond traditional, document-based traceability systems. Its objective nature could help minimize the risks of errors, fraud, or mislabeling, potentially ensuring a credible and transparent verification process for HPP treatments that supports product quality and safety. In the context of official controls, the methodology might also benefit competent authorities. It could provide an objective and scientifically validated verification method to strengthen the certification of HPP treatment execution, which in turn may facilitate compliance with export requirements and support the global distribution of products. Furthermore, for international regulators, this approach might represent a reliable means to verify that imported meat products have undergone the declared HPP treatment, thus addressing concerns related to authenticity and compliance with food safety standards.

Nevertheless, to fully exploit the potential of the proposed methodology, future efforts should focus on improving its applicability to meat products with greater structural variability. This is particularly relevant for pressed hams, for which less satisfactory classification performance was observed. To overcome this current limitation, further studies should include larger and more heterogeneous sample sets and evaluate the method across a broader range of production batches. In addition, longer-term investigations are needed to assess stability and robustness over extended storage periods and under varying commercial conditions, thereby further supporting its implementation in real-world settings. Once these challenges are addressed, exploring the scalability of the method to other food matrices and processing conditions will also be essential. Ultimately, such advancements could position NIR spectroscopy as a practical tool within modern food safety management systems, providing a versatile, rapid, and non-destructive solution for verifying food processing and ensuring product integrity across the global food supply network.

CRediT authorship contribution statement

Emanuela Zanardi: Writing – review & editing, Writing – original draft, Project administration, Conceptualization. **Maria Olga Varrà:** Writing – original draft, Methodology, Conceptualization. **Alessandra Negri:** Visualization, Validation, Investigation. **Riccardo Ghidini:** Validation, Resources, Investigation. **Riccardo Soldesti:** Visualization, Validation, Resources, Investigation. **Adriana Ianieri:** Writing – review & editing, Visualization, Resources. **Sergio Ghidini:** Writing – review & editing, Project administration, Conceptualization.

Funding

This work was supported by the University of Parma (Italy) and carried out within the framework of the ALIFAR project, supported by the Italian Ministry of University and Research (MUR) through the "Dipartimenti di Eccellenza 2023–2027" program.

Declaration of competing interest

The authors declare that they have no known competing financial interests or personal relationships that could have appeared to influence the work reported in this paper.

Acknowledgements

The authors acknowledge Giovanni Tommaso Lanza and Davide Vecchi for their contribution to recording part of the raw NIR spectra during the early stages of evaluating the applicability of the methodology.

Appendix B. Supplementary data

Supplementary data to this article can be found online at https://doi.org/10.1016/j.foodcont.2025.111946.

Appendix A. Supplementary materials

The following are the Supplementary data to this article:

Data availability

Data will be made available on request.

References

Arias, E., Sierra, V., Prado, N., González, P., Fiorentini, G., Díaz, J., & Oliván, M. (2022). Development of a portable near-infrared spectroscopy tool for detecting freshness of commercial packaged pork. *Foods, 11*(23). https://doi.org/10.3390/foods11233808. Article 3808.

Aymerich, T., Picouet, P. A., & Monfort, J. M. (2008). Decontamination technologies for meat products. *Meat Science, 78*(1–2), 114–129. https://doi.org/10.1016/j.meatsci.2007.07.007

Bajovic, B., Bolumar, T., & Heinz, V. (2012). Quality considerations with high pressure processing of fresh and value-added meat products. *Meat Science, 92*(3), 280–289. https://doi.org/10.1016/j.meatsci.2012.04.024

Barba, F. J., Terefe, N. S., Buckow, R., Knorr, D., & Orlien, V. (2015). New opportunities and perspectives of high pressure treatment to improve health and safety attributes of foods. A review. *Food Research International, 77*, 725–742. https://doi.org/10.1016/j.foodres.2015.05.015

Beć, K. B., Grabska, J., & Huck, C. W. (2020a). Principles and applications of miniaturized near-infrared (NIR) spectrometers. *Chemistry - A European Journal, 27*(5), 1514–1532. https://doi.org/10.1002/chem.202002838

Beć, K. B., Grabska, J., & Huck, C. W. (2020b). Near-infrared spectroscopy in bio-applications. *Molecules, 25*(12), 2948. https://doi.org/10.3390/molecules25122948

Bolumar, T., Orlien, V., Sikes, A., Aganovic, K., Bak, K. H., Guyon, C., Stübler, A. S., de Lamballerie, M., Hertel, C., & Brüggemann, D. A. (2021). High-pressure processing of meat: Molecular impacts and industrial applications. *Comprehensive Reviews in Food Science and Food Safety, 20*(1), 332–368. https://doi.org/10.1111/1541-4337.12670

Cáceres-Nevado, J. M., Garrido-Varo, A., De Pedro-Sanz, E., & Pérez-Marín, D. C. (2019). Fourier transform near-infrared spectroscopy coupled to a long fibre optic head for the quality control of Iberian pork loins: Intact versus minced. *Meat Science, 153*, 86–93. https://doi.org/10.1016/j.meatsci.2019.03.008

Campus, M., Flores, M., Martinez, A., & Toldrá, F. (2008). Effect of high pressure treatment on colour, microbial and chemical characteristics of dry cured loin. *Meat Science, 80*(4), 1174–1181. https://doi.org/10.1016/j.meatsci.2008.05.011

Collell, C., Gou, P., Arnau, J., & Comaposada, J. (2011). Non-destructive estimation of moisture, water activity and NaCl at ham surface during resting and drying using NIR spectroscopy. *Food Chemistry, 129*(2), 601–607. https://doi.org/10.1016/j.foodchem.2011.04.073

De Marchi, M., Manuelian, C. L., Ton, S., Manfrin, D., Meneghesso, M., Cassandro, M., & Penasa, M. (2017). Prediction of sodium content in commercial processed meat products using near infrared spectroscopy. *Meat Science, 125*, 61–65. https://doi.org/10.1016/j.meatsci.2016.11.014

de Oliveira, F. A., Neto, O. C., dos Santos, L. M. R., Ferreira, E. H. R., & Rosenthal, A. (2017). Effect of high pressure on fish meat quality–A review. *Trends in Food Science & Technology, 66*, 1–19. https://doi.org/10.1016/j.tifs.2017.04.014

European Commission. (2004). Regulation (EC) no. 852/2004 of the European Parliament and of the council of 29 April 2004 on the hygiene of foodstuffs. *Official Journal of the European Communities - Legislation, 139/1*. https://eur-lex.europa.eu/legal-content/EN/TXT/HTML/?uri=CELEX:32004R0852.

Fernández-Barroso, M.Á., Parrini, S., Muñoz, M., Palma-Granados, P., Matos, G., Ramírez, L., Crovetti, A., García-Casco, J. M., & Bozzi, R. (2021). Use of NIRS for the assessment of meat quality traits in open-air free-range Iberian pigs. *Journal of Food Composition and Analysis, 102*, Article 104018. https://doi.org/10.1016/j.jfca.2021.104018

Fuentes, V., Ventanas, J., Morcuende, D., Estévez, M., & Ventanas, S. (2010). Lipid and protein oxidation and sensory properties of vacuum-packaged dry-cured ham subjected to high hydrostatic pressure. *Meat Science, 85*(3), 506–514. https://doi.org/10.1016/j.meatsci.2010.02.024

Fulladosa, E., Serra, X., Gou, P., & Arnau, J. (2009). Effects of potassium lactate and high pressure on transglutaminase restructured dry-cured hams with reduced salt content. *Meat Science, 82*(2), 213–218. https://doi.org/10.1016/j.meatsci.2009.01.013

Galindo-Prieto, B., Eriksson, L., & Trygg, J. (2015). Variable influence on projection (VIP) for OPLS models and its applicability in multivariate time series analysis. *Chemometrics and Intelligent Laboratory Systems, 146*, 297–304. https://doi.org/10.1016/j.chemolab.2015.05.001

Georget, E., Sevenich, R., Reineke, K., Mathys, A., Heinz, V., Callanan, M., Rauh, C., & Knorr, D. (2015). Inactivation of microorganisms by high isostatic pressure processing in complex matrices: A review. *Innovative Food Science & Emerging Technologies, 27*, 1–14. https://doi.org/10.1016/j.ifset.2014.10.015

González-Mohino, A., Pérez-Palacios, T., Antequera, T., Ruiz-Carrascal, J., Olegario, L. S., & Grassi, S. (2020). Monitoring the processing of dry fermented sausages with a portable NIRS device. *Foods, 9*(9), Article 1294. https://doi.org/10.3390/foods9091294

Grossi, A., Olsen, K., Bolumar, T., Rinnan, Å., Øgendal, L. H., & Orlien, V. (2016). The effect of high pressure on the functional properties of pork myofibrillar proteins. *Food Chemistry, 196*, 1005–1015. https://doi.org/10.1016/j.foodchem.2015.10.062

Hassoun, A., Ojha, S., Tiwari, B., Rustad, T., Nilsen, H., Heia, K., Cozzolino, D., Bekhit, A. A., Biancolillo, A., & Wold, J. P. (2020). Monitoring thermal and non-thermal treatments during processing of muscle foods: A comprehensive review of recent technological advances. *Applied Sciences, 10*(19), Article 6802. https://doi.org/10.3390/app10196802

Hereu, A., Bover-Cid, S., Garriga, M., & Aymerich, T. (2011). High hydrostatic pressure and biopreservation of dry-cured ham to meet the food safety objectives for *Listeria monocytogenes*. *International Journal of Food Microbiology, 154*(3), 107–112. https://doi.org/10.1016/j.ijfoodmicro.2011.02.027

Hernández-Jiménez, M., Revilla, I., Vivar-Quintana, A. M., Grabska, J., Beć, K. B., & Huck, C. W. (2024). Comparison of miniaturized and benchtop NIR spectrophotometers for quantifying the fatty acid profile of Iberian ham. *Applied Sciences, 14*(22), Article 10680. https://doi.org/10.3390/app142210680

Italian Ministry of Health. (2022). Note n. 0012715-29/03/2022-DGISAN-MDP-P of 29 March 2022. *Trattamenti di Alte Pressioni (HPP – High Pressure Processing) in prodotti alimentari destinati all'esportazione verso gli USA ed altri Paesi Terzi* (aggiornamento NOTA DGISAN_30836 DEL 29_07_2016).

EFSA Panel on Biological Hazards (BIOHAZ Panel), Koutsoumanis, K., Alvarez-Ordóñez, A., Bolton, D., Bover-Cid, S., Chemaly, M., Davies, R., De Cesare, A., Herman, L., Hilbert, F., Lindqvist, R., Nauta, M., Peixe, L., Ru, G., Simmons, M., Skandamis, P., Suffredini, E., Castle, L., Crotta, M., Grob, K., Milana, M. R., Petersen, A., Roig Sagués, A. X., Vinagre Silva, F., Barthélémy, E., Christodoulidou, A., Messens, W., & Allende, A. (2022). The efficacy and safety of high-pressure processing of food. *EFSA Journal, 20*(3), Article e07128. https://doi.org/10.2903/j.efsa.2022.7128

León, L., Ortiz, A., Ezquerro, S., & Tejerina, D. (2023). NIRS (Near Infrared Spectroscopy) classification of sliced duroc dry-cured ham under various packaging systems and storage temperature and time. *Meat Science, 206*, Article 109348. https://doi.org/10.1016/j.meatsci.2023.109348

McArdle, R. A., Marcos, B., Kerry, J. P., & Mullen, A. M. (2011). Influence of HPP conditions on selected beef quality attributes and their stability during chilled storage. *Meat Science, 87*(3), 274–281. https://doi.org/10.1016/j.meatsci.2010.10.022

McArdle, R. A., Marcos, B., Mullen, A. M., & Kerry, J. P. (2013). Influence of HPP conditions on selected lamb quality attributes and their stability during chilled storage. *Innovative Food Science & Emerging Technologies, 19*, 66–72. https://doi.org/10.1016/j.ifset.2013.04.003

Mungkarndee, R., Techakriengkrai, I., Tumcharern, G., & Sukwattanasinitt, M. (2016). Fluorescence sensor array for identification of commercial milk samples according to their thermal treatments. *Food Chemistry, 197*(Part A), 198–204. https://doi.org/10.1016/j.foodchem.2015.10.083

Niemeyer, S., Wacker, R., & Kunz, A. (2010). Influence of derivative processing and spectral resolution on the interpretation of near-infrared spectra for chemical analysis. *Analytica Chimica Acta, 661*(1), 24–32. https://doi.org/10.1016/j.aca.2009.10.035

Patazca, E., Koutchma, T., & Balasubramaniam, V. M. (2007). Quasi-adiabatic temperature increase during high pressure processing of selected foods. *Journal of Food Engineering, 80*, 199–205. https://doi.org/10.1016/j.jfoodeng.2006.05.014

Pavli, F., Argyri, A. A., Nychas, G. J., Tassou, C., & Chorianopoulos, N. (2018). Use of fourier transform infrared spectroscopy for monitoring the shelf life of ham slices packed with probiotic supplemented edible films after treatment with high pressure processing. *Food Research International, 106*, 1061–1068. https://doi.org/10.1016/j.foodres.2017.12.064

Pérez-Santaescolástica, C., Carballo, J., Fulladosa, E., Munekata, P. E. S., Campagnol, P. B., Gómez, B., & Lorenzo, J. M. (2019). Influence of high-pressure processing at different temperatures on free amino acid and volatile compound profiles of dry-cured ham. *Food Research International, 116*, 49–56. https://doi.org/10.1016/j.foodres.2018.12.039

Petrini, S., Brutti, A., Casciari, C., Calderone, D., Pela, M., Giammarioli, M., Righi, C., & Feliziani, F. (2024). High-pressure processing of different tissue homogenates from pigs challenged with the African swine fever virus. *Viruses, 16*(4). https://doi.org/10.3390/v16040638. Article 638.

Picouet, P. A., Sala, X., Garcia-Gil, N., Nolis, P., Colleo, M., Parella, T., & Arnau, J. (2012). High pressure processing of dry-cured ham: Ultrastructural and molecular changes affecting sodium and water dynamics. *Innovative Food Science & Emerging Technologies, 16*, 335–340. https://doi.org/10.1016/j.ifset.2012.07.008

Prieto, N., Roehe, R., Lavin, P., Batten, G., & Andres, S. (2009). Application of near infrared reflectance spectroscopy to predict meat and meat products quality: A review. *Meat Science, 83*, 175–186. https://doi.org/10.1016/j.meatsci.2009.04.016

Rasanayagam, V., Balasubramaniam, V. M., Ting, E., Sizer, C. E., Bush, C., & Anderson, C. (2003). Compression heating of selected fatty food materials during high-pressure processing. *Journal of Food Science, 68*, 254–259. https://doi.org/10.1111/j.1365-2621.2003.tb14148.x

Reiner, J., Protte, K., & Hinrichs, J. (2020). Investigation of the applicability of raman spectroscopy as online process control during consumer milk production. *Chemical Engineering, 4*(3). https://doi.org/10.3390/chemengineering4030045. Article 45.

Ritthiruangdej, P., Ritthiron, R., Shinzawa, H., & Ozaki, Y. (2011). Non-destructive and rapid analysis of chemical compositions in Thai steamed pork sausages by near-infrared spectroscopy. *Food Chemistry, 129*(2), 684–692. https://doi.org/10.1016/j.foodchem.2011.04.110

Rubio-Celorio, M., Fulladosa, E., García-Gil, N., & Bertram, H. C. (2016). Multiple spectroscopic approach to elucidate water distribution and water-protein interactions in dry-cured ham after high pressure processing. *Journal of Food Engineering, 169*, 291–297. https://doi.org/10.1016/j.jfoodeng.2015.09.008

Schmutzler, M., Beganovic, A., Böhler, G., & Huck, C. W. (2015). Methods for detection of pork adulteration in veal product based on FT-NIR spectroscopy for laboratory, industrial and on-site analysis. *Food Control, 57*, 258–267. https://doi.org/10.1016/j.foodcont.2015.04.019

Simonin, H., Duranton, F., & De Lamballerie, M. (2012). New insights into the high-pressure processing of meat and meat products. *Comprehensive Reviews in Food Science and Food Safety, 11*(3), 285–306. https://doi.org/10.1111/j.1541-4337.2012.00184.x

Sun, X. D., & Holley, R. A. (2010). High hydrostatic pressure effects on the texture of meat and meat products. *Journal of Food Science, 75*(1), R17–R23. https://doi.org/10.1111/j.1750-3841.2009.01449.x

Tejerina, D., Contador, R., & Ortiz, A. (2021). Near infrared spectroscopy (NIRS) as tool for classification into official commercial categories and shelf-life storage times of pre-sliced modified atmosphere packaged iberian dry-cured loin. *Food Chemistry, 356*, Article 129733. https://doi.org/10.1016/j.foodchem.2021.129733

Tintchev, F., Bindrich, U., Toepfl, S., Strijowski, U., Heinz, V., & Knorr, D. (2013). High hydrostatic pressure/temperature modeling of frankfurter batters. *Meat Science, 94*(3), 376–387. https://doi.org/10.1016/j.meatsci.2013.02.012

Varrà, M. O., Fasolato, L., Serva, L., Ghidini, S., Novelli, E., & Zanardi, E. (2020). Use of near infrared spectroscopy coupled with chemometrics for fast detection of irradiated dry fermented sausages. *Food Control, 110*, Article 107009. https://doi.org/10.1016/j.foodcont.2019.107009

Workman, J. J., & Weyer, L. (2012). *Practical guide and spectral atlas for interpretive near-infrared spectroscopy* (2nd ed.). CRC Press.

Yazgan, N. N., Genis, H. E., Bulat, T., Topcu, A., Durna, S., Yetisemiyen, A., & Boyaci, I. H. (2020). Discrimination of milk species using raman spectroscopy coupled with partial least squares discriminant analysis in raw and pasteurized milk. *Journal of the Science of Food and Agriculture, 100*(13), 4756–4765. https://doi.org/10.1002/jsfa.10534